

A NEW APPROACH TO MODELING A MICROWAVE ANTENNA ARRAY WITH A PHASE RADIATION PATTERN

Elmar Hunbataliyev*

Department of Radio Engineering and Telecommunication, Faculty of Information and Telecommunication Technology, Azerbaijan Technical University, H. Javid ave 25, AZ 1073, Baku, Azerbaijan

ARTICLE INFO:

Article history:

Received: 09.06.2023.

Received in revised form: 12.01.2024.

Accepted: 21.03.2024.

Keywords:

Antenna array

Microwave

Side lobe level

Radiation pattern

Directional factor

DOI: <https://doi.org/10.30765/er.2277>

Abstract:

In this paper, models of an annular antenna array have been developed and an analysis of the main characteristics of this antenna array has been carried out. The obtained results suggest that the considered variants of the microwave ring antenna array with discrete-switching scanning of the azimuthal radiation patterns, taking into account the weight, size and electrical characteristics, seem promising for use in the equipment of radio communication, radar and radio control systems. And also a method for correcting the distortions of the directional patterns of the developed annular antenna array, caused by the mutual influence of emitters, is proposed. To implement this technique, an algorithm has been developed for changing the amplitude distribution of the electromagnetic field strength from the phase distribution of the electromagnetic field strength to compensate for the distortion of parameters caused by the deviation of the beam of the radiation pattern.

1 Introduction

At present, various technical means and systems are widely used in various spheres of life, among which, within the framework of this article, radio-controlled unmanned vehicles of various bases are distinguished, on the one hand, and radio systems of broadband wireless access of the Wi-Max standard, on the other hand. The interest in these seemingly completely different means and systems is due to the fact that radio channels are used both in radio control systems for unmanned vehicles and in radio systems for broadband wireless access. Therefore, the reliability and quality of operation of these systems significantly depend on the characteristics of not only the actual transceiver radio equipment, but also the antenna-feeder devices - the shape and parameters of radiation patterns, gain factors and the ability to control antenna radiation patterns. In the equipment of control and communication systems with unmanned aerial vehicles and broadband wireless access systems, various antennas are used, both with circular, sector and needle-shaped radiation patterns fixed in space, and with electrically controlled radiation patterns. Increasing requirements for weight, size and cost parameters of control and communication systems equipment, bandwidth, noise immunity and noise immunity of these systems, and their functionality dictate the need for continuous improvement of antenna technology. In this regard, of particular interest for research are ring antenna arrays, which make it possible to form circular, multibeam, fixed, and scanning sector radiation patterns, due to which, in a number of applications, antennas with fixed radiation patterns can be successfully replaced.

The purpose of this work was to develop and study a microwave ring antenna array with electric scanning of azimuthal radiation patterns, intended for use in equipment systems of fixed and mobile broadband wireless access, as well as systems of radio control and communication with unmanned vehicles. The circular antenna arrays discussed below were developed for the frequency band 3,4-3,7 GHz. First of all, this concerns the development of relatively simple mathematical models of the antenna array for illumination signals with vertical and horizontal polarization, which would allow the developer to determine the distortions of the phase

* Corresponding author

E-mail address: elmarzulfugar59@gmail.com

and amplitude radiation patterns depending on the design parameters of the array and thereby help choose the optimal design solution for the antenna array. Accurate electrodynamic modeling, which requires large computational resources and time, can only be used to verify the solution found. New fundamental research in the field of circuitry and design solutions for emitters for broadband antenna arrays operating with vertical and horizontal polarizations of the illumination signal does not fully satisfy developers, since they often have a narrow band and provide greater unevenness of the antenna array radiation patterns, which reduces the accuracy of determining the bearing to the target. Therefore, it seems relevant to search for new technical solutions for emitters of various frequency ranges operating in a wide band with vertical and horizontal polarization for use in an antenna array, and to evaluate their characteristics as part of the arrays. Naturally, it is necessary to develop experimental samples of emitters and antenna arrays based on them, study them and check the coincidence of theoretical and experimental characteristics. The present work is devoted to solving these current problems. An annular antenna array can be represented as a variant of a cylindrical antenna array containing only one floor of emitters (Figure 1). The antenna array radius is 100 mm , the reflector radius is 85 mm , the reflector height is 50 mm and the screen radius is 135 mm .

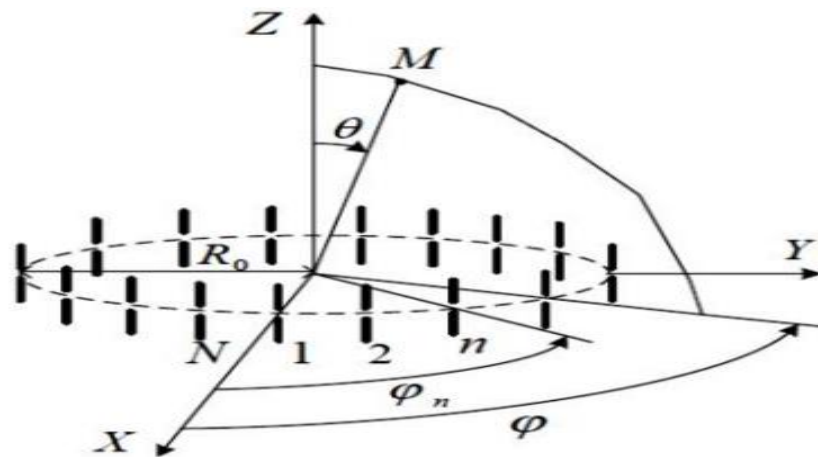


Figure 1. Ring antenna array.

2 Formulation of the problem

For electrical scanning of the radiation patterns of a conventional passive annular antenna array in the azimuth plane, the following is usually used: phasing of the emitter fields in a given direction using phase shifters in phased antenna arrays [1-5] and with the help of special matrix or lens beamforming systems in multibeam antenna arrays [6-9], selective excitation of radiators in annular antenna arrays with discrete switching scanning. Further, two variants of passive ring microwave antenna arrays are considered: with phase scanning of radiation patterns using controlled phase shifters, Figure 2 (a); with discrete-switching scanning using switches built on the basis of power dividers/combiners with switches, Figure 2 (b). Due to circular symmetry, ring antenna arrays make it possible to obtain almost circular (in the plane of the array) radiation patterns, as well as to form a scanning sector or even needle-shaped radiation patterns, the shape of which can be maintained unchanged when scanning in the XOY plane within 360° [10-14]. Microwave circular phased antenna arrays can provide circular scanning of radiation patterns with a very small angular step [15-17]. At the same time, traditional phased antenna arrays also have serious drawbacks - high thermal losses in semiconductor microwave phase shifters, which limit the efficiency and gain of phased antenna arrays, as well as the complexity of the control system [18-21]. Ring antenna arrays with discrete-switching pattern scanning are characterized by a simpler control system, lower heat losses in the switch, respectively, higher efficiency and gain, but provide discrete scanning of pattern patterns with a certain angular step, depending on the number of array elements. However, this is not an obstacle to the use of such annular antenna arrays in many real control and communication systems [22-25].

This article presents the results of the development and simulation of two variants of microwave ring antenna arrays: 8- and 16-element low-profile ring antenna arrays from vertical asymmetric vibrators and an 8-element ring antenna array composed of linear strip antenna arrays. Ring antenna arrays were calculated to

obtain an azimuthal gain of at least 6-8 dB [26]. The vibrator ring microwave antenna array is shown in Figure 3, which indicates: 1 - screen; 2 - cylindrical reflector; 3 - emitter; 4 - coaxial connector; R_e is the screen radius; R_p and H_p are the radius and height of the reflector; R_i is the distance from the origin of coordinates to the vertical axis of the emitter; H_i is the height of the emitter; θ and φ are the meridional and azimuthal angles that determine the direction to the observation point M (M' is the projection of the point M onto the horizontal plane XOY).

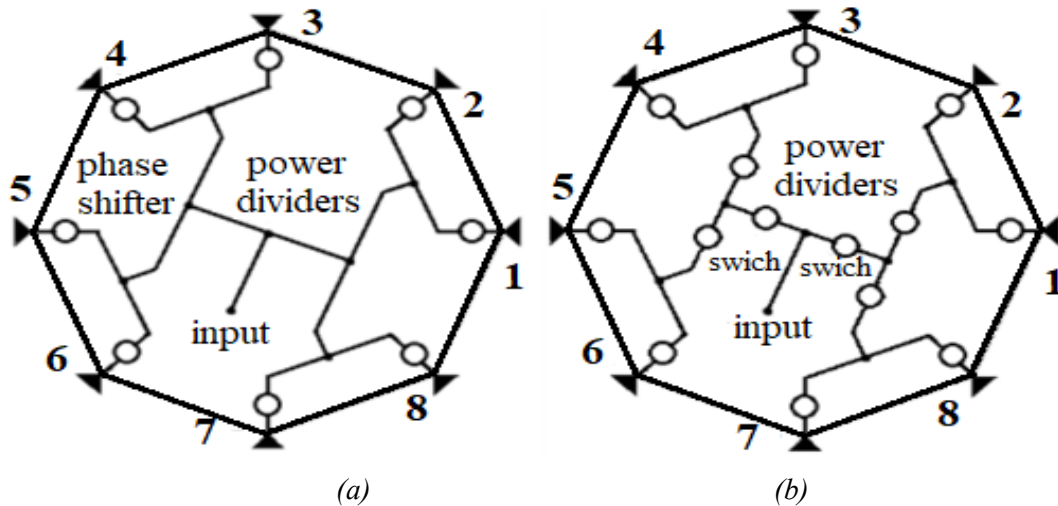


Figure 2. Structures of passive ring antenna arrays with parallel power division with (a) phase and (b) discrete-switching scanning.

For a given antenna array, an important aspect is knowledge of the input characteristics. In linear or flat antenna arrays with common-mode radiation, the input impedance of the emitters is the same. A change in the input resistance occurs when the beam swings (with a linear change in the phase front), thereby changing the standing wave coefficient at their inputs. The greater the beam deviation, the greater the mismatch with the supply transmission line, which, in principle, limits the scanning sector. In cylindrical antenna arrays, uneven input impedance of the emitters is present initially due to the specifics of beam focusing. And beam scanning can be carried out by rotating the exciting sector. Since the input impedances of the emitters in the excitation sector turn out to be different and differ (sometimes significantly) from the wave impedance of the supply transmission lines, then in order to minimize energy losses, the problem arises of optimizing the value of this wave impedance. In terms of practical implementation, this means that a transforming device must be added to the input of each emitter.

It can be seen that in the “off” state the screen reflects the field of the antenna array emitters, $|S_{11}| > -0,5$ dB in the frequency band around 1,6 GHz (8 GHz to 9,6 GHz). In the “on” state, the screen transmits the radiation field, $|S_{11}| < -13$ dB in the frequency band 8–12 GHz. In this case, the value $|S_{11}|$ depends significantly on the distance between the frequency-selective surface and the antenna array. Better antenna array matching is achieved if the frequency-selective surface is in close proximity to the aperture. The design parameters of the annular antenna array were calculated according to the method described in [27, 28], taking into account the fact that, for example, when discrete scanning of radiation patterns in the azimuthal plane with an angular step of $22,5^\circ$, the width of the radiation patterns $\varphi_{0,5}$ must be at least $22,5^\circ$ to overlap radiation patterns in adjacent angular directions at a level not exceeding -3 dB.

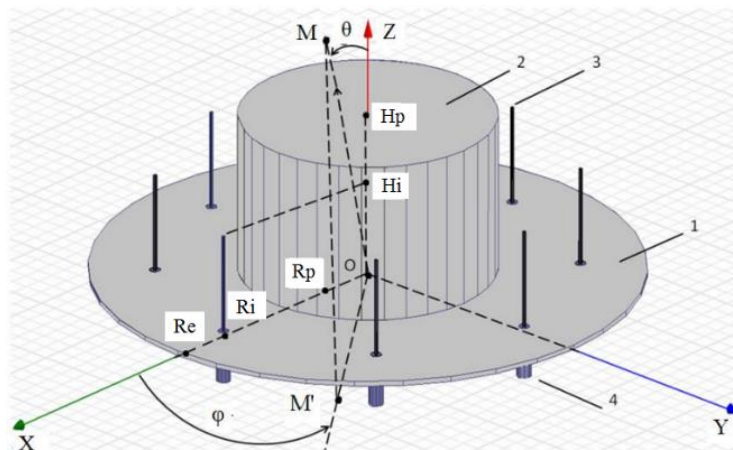


Figure 3. Vibrator ring antenna array.

As a result, it was found that $R_i=47\text{ mm}$, the circumference on which the elements of the annular antenna array are located $L=295\text{ mm}$, and the number of emitters N , taking into account the distance between them, is not more than $\Delta L=\lambda_{min}/2$ (λ_{min} is the minimum operating wavelength, at a frequency of $3,6\text{ GHz}$ equal to $83,3\text{ mm}$) $N=L/\Delta L=7$. For the convenience of building a parallel power supply circuit for the elements of an annular antenna array, the number of elements has been increased to 8.

3 Phase scanning of the radiation pattern

As an example, let's consider two versions of an annular antenna array of vertical radiators: with circular and cardioid azimuthal radiation patterns. On Figure 4 shows the normalized radiation patterns of the annular antenna array at an average operating frequency of $3,5\text{ GHz}$ for the zero azimuth direction, calculated assuming equal-amplitude excitation of radiators according to the formulas given in [29] (calculated values of the phases of the currents F1-8 in the elements of the annular antenna array at $0^\circ, 58^\circ, 197^\circ, 337^\circ, 395^\circ, 337^\circ, 197^\circ, 58^\circ$). As can be seen from Figure 4, the azimuthal radiation patterns of both versions of the annular array are quite narrow (about 32° wide), but have a high level of the side lobe, in particular, the back lobe: about -5 dB . As expected, during phase scanning of radiation patterns in the case of equal-amplitude excitation, both versions of the annular antenna array have radiation patterns with a high level of side lobes, which is unacceptable in terms of providing high noise immunity of the receiving channel and low level of side radiation of the transmitting channel of the control or communication system.

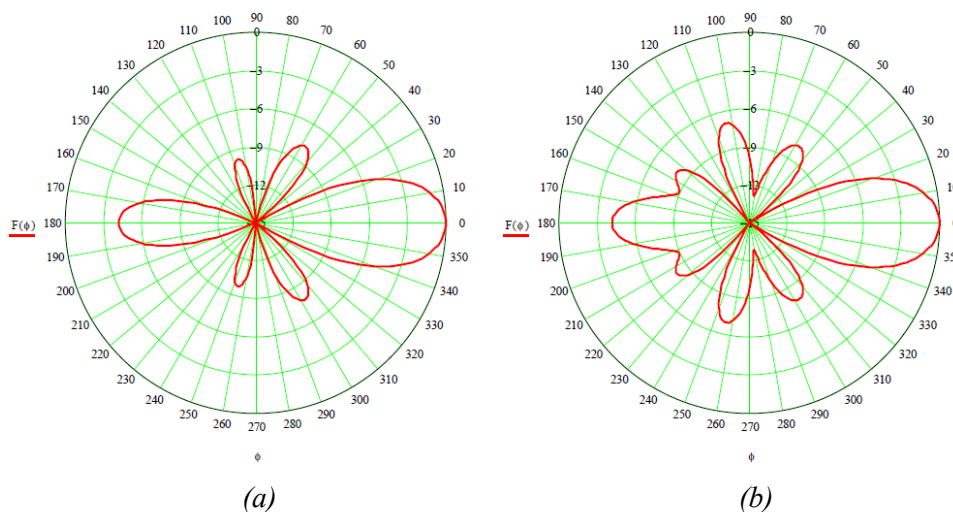


Figure 4. Examples of directivity patterns of an annular antenna array: from emitters with circular radiation patterns (a) and with cardioid radiation patterns (b).

Of course, the level of the side lobes of the radiation patterns can be reduced in the case of uneven excitation of the elements of the annular antenna array [3, 4], but this will require a significant complication of the beam-forming system and will lead to a decrease in the radiation power of the antenna.

4 Discrete-switching beam pattern scanning

On Figure 5 shows the radiation patterns of an eight-element annular antenna array of radiators with cardioid radiation patterns, calculated when one and two adjacent radiators of the annular antenna array are excited by currents of the same amplitude and phase.

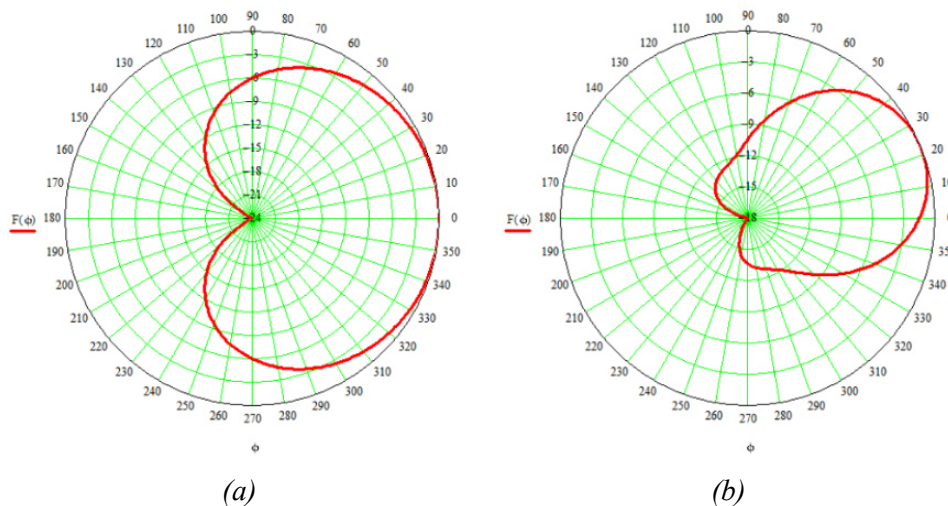


Figure 5. Examples of radiation patterns of an annular antenna array: with one active radiator (a) and two adjacent active radiators (b).

As can be seen from Figure 5, in the case of one excited radiator, the width of the radiation patterns is 134° , and in the case of two excited radiators, it is 66° and has deep dips in the rear direction. In the case of three excited radiators, the radiation pattern narrows to 54° , which leads to an increase in the directivity of the annular antenna array, but this significantly complicates the control circuit of the array. Thus, for practical use in the scanning mode of sectoral radiation patterns, a ring antenna array with discrete switching scanning in the mode of excitation of pairs of adjacent radiators seems to be more attractive, especially since the heat losses in microwave switches turn out to be several decibels less than in phase shifters.

5 Simulation modelling of an 8-element vibrator ring antenna array with discrete-switching beam pattern scanning

Parameters of the ring antenna array model: calculated value of the grating radius for the average frequency of $3,5 \text{ GHz}$ $R_i = 47 \text{ mm}$; distance from the reflector to the vertical axis of the emitter ($\lambda_{min}/4$) 21 mm ; reflector radius $R_p = 26 \text{ mm}$; distance from the vertical axis of the emitter to the edge of the screen ($\lambda_{min}/4$) 21 mm ; screen radius $R_e = 68 \text{ mm}$; reflector height H_p is taken equal to $1,2 \lambda_{min}/4 = 31,5 \text{ mm}$. Rated input impedance of vibrator elements is 50 Ohm . The simulation was performed using the HFSS program. On Figure 6 shows the frequency characteristics of the active standing wave ratio of a pair of adjacent active elements of the annular antenna array (matched loads are connected to the inputs of the rest). In this case, the minimum standing wave ratio = $1,07$ is achieved at the average operating frequency, and in the frequency band $3,36\text{-}3,68 \text{ GHz}$, the standing wave ratio does not exceed $1,5$.

The radiation patterns of an annular antenna array in the case of a pair of active elements (1 and 2) are shown in Figure 7. According to the azimuth radiation patterns in Figure 7 (a) it can be seen that the value of the width of the radiation patterns is approximately 65° , which is quite enough to overlap the radiation patterns in neighboring azimuth directions when scanning at a gain level of at least $4,5 \text{ dB}$. In this case, the gain of the annular antenna array in the azimuthal plane is $6,2 \text{ dB}$, the maximum value ($7,2 \text{ dB}$) is achieved at an elevation angle of 26° , Figure 7 (b).

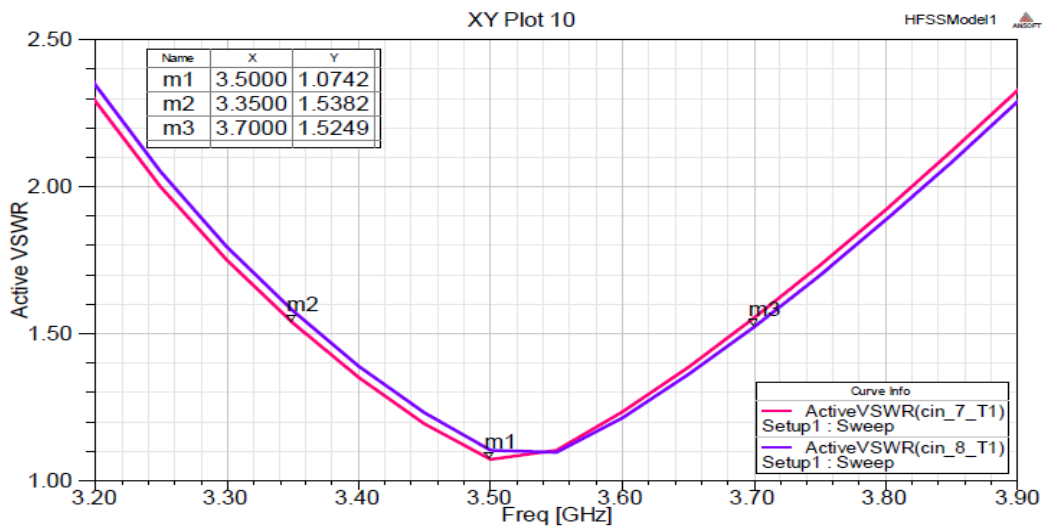


Figure 6. Frequency characteristics of the active standing wave coefficient at the inputs of two adjacent active elements of the annular antenna array.

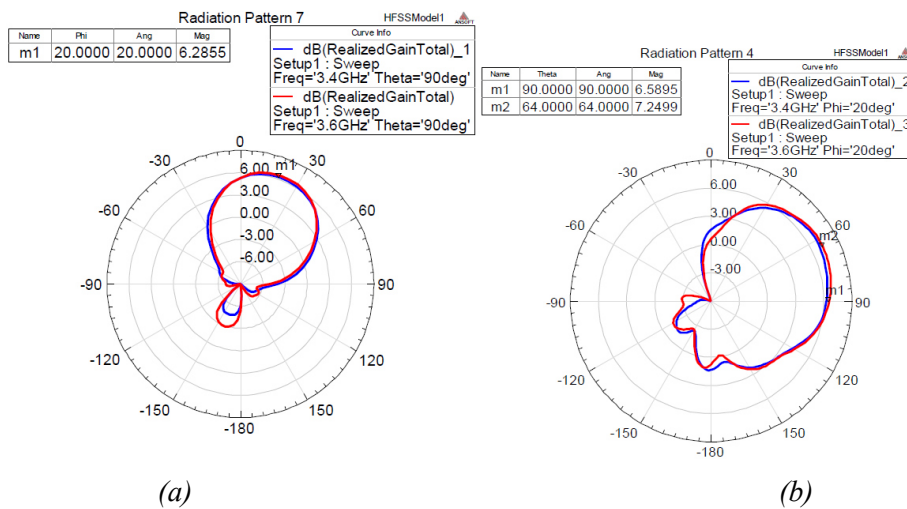


Figure 7. Azimuthal (a) and meridional (b) radiation patterns of an annular antenna array at frequencies of 3,4 and 3,6 GHz for the case of two active elements.

6 Simulation modelling of a 16-element vibrator ring antenna array with discrete-switching beam pattern scanning

To increase the gain and the number of discrete positions of the radiation patterns in the azimuth plane, a 16-element annular antenna array was developed. The results of modeling a 16-element annular antenna array from the same vertical vibrators, obtained with an array radius of 100 mm, a reflector radius of 85 mm, a reflector height of 50 mm, and a screen radius of 135 mm, are shown in Figure 8 and 9. In Figure 8 shows the frequency characteristics of the active standing wave ratio of a pair of adjacent elements of the annular antenna array (matched loads are connected to the inputs of the rest). In this case, the minimum standing wave ratio = 1,06 is achieved at a frequency of 3,45 GHz, and in the band 3,3-3,65 GHz the standing wave ratio does not exceed 1,5.

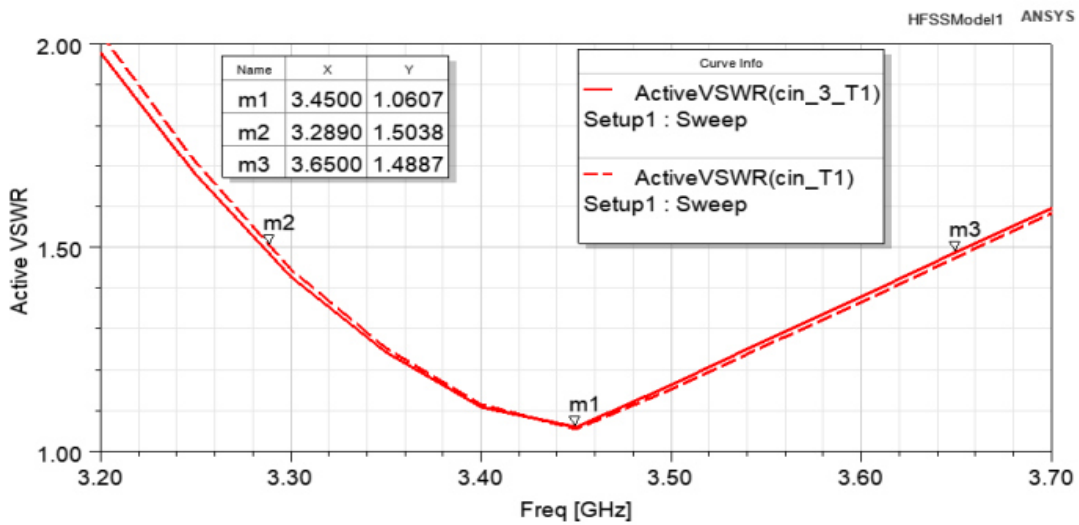


Figure 8. Frequency characteristics of the active standing wave coefficient at the inputs of a pair of neighboring active elements of the annular antenna array.

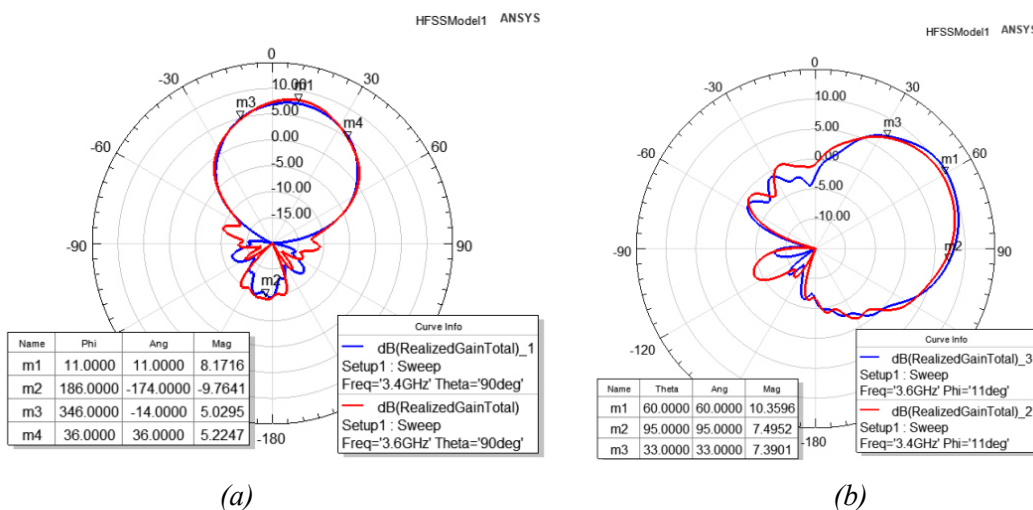


Figure 9. Azimuthal (a) and meridional (b) radiation patterns of an annular antenna array at frequencies of 3,4 and 3,6 GHz for the case of a pair of active elements.

From Figure 9 (a) it can be seen that the width of the radiation patterns is 50° , which is quite enough to overlap the radiation patterns in a pair of adjacent 16 azimuthal directions with a gain of at least 6 dB, in this case, the gain of the annular antenna array in the azimuthal plane exceeds 8 dB, and its maximum value (10 dB) achieved at 30° elevations; the level of the side lobes of the radiation patterns does not exceed -17 dB. The width of the radiation patterns in the meridional plane is approximately 62° , the level of the side lobes of the radiation patterns does not exceed -10 dB. Modeling an annular array with four or more active radiators showed that the directivity and gain do not increase, but decrease due to the deterioration in the shape of the directivity patterns (increase in the level of side lobes). Based on the results obtained, it can be concluded that the vibrator ring antenna arrays discussed above can be used as a subscriber terminal antenna in the mobile Wi-Max system to ensure the retention of radiation patterns in the direction to the base station, in the equipment of the control system for ground and air unmanned aerial vehicles of small radius actions at relatively small required values of the antenna gain. In cases where antennas with a gain above 8-10 dB and a low level of lateral radiation are needed, it is advisable to use annular antenna arrays from vertical antenna arrays that provide narrowing of the radiation patterns in the meridional planes and, respectively, an increase in the directivity and gain.

7 Strip ring antenna array

The microwave strip ring antenna array, also designed for the 3,4-3,6 GHz frequency band, was designed to achieve a gain of at least 14 dB in the scanning sector pattern mode. For this purpose, the annular antenna array is composed of eight elements in the form of linear antenna arrays such as sectoral collinear antennas, Figure 10, which indicates: 1 - strip collinear antenna in the form of a two-sided linear array of twelve rectangular patches, 2 - reflector, 3 - metal base of the antenna with a coaxial-strip transition. The dimensions of the design of a single element of the annular antenna array: $A=30\text{ mm}$, $B=375\text{ mm}$, $R=22\text{ mm}$; dimensions of the annular array structure: height 375 mm, base diameter 300 mm. In the model under consideration, a 0,51 mm thick substrate made of a dielectric material with a relative permittivity of 3,55 and a dielectric loss tangent of 0,0027 was used in the design of strip antennas. The linear strip array has a constant patch spacing, and the width of each patch is determined by the method of optimizing the designs of the antennas of the leaky wave [4] in such a way that along the vertical axis of the array to realize the amplitude distribution of the “sine on a pedestal” type, which theoretically provides the level of side lobe radiation patterns not higher than -20 dB at a sufficiently high utilization factor of the grating length [1, 2]. The nominal input impedance of each grating is 50 Ohms.

The frequency characteristics of the active standing wave coefficient for all eight inputs of the annular antenna array, obtained for the case of their equal-amplitude in-phase excitation, are shown in Figure 11. The maximum standing wave ratio in the frequency band 3,4-3,6 GHz does not exceed 1,8. Examples of the radiation patterns of an annular antenna array, obtained as a result of simulation in the mode of forming a scanning sector radiation pattern, are shown in Figure 12. An annular antenna array provides switching of directional patterns in eight azimuth directions with an angular step of 45° and overlapping of the main lobes of the directional patterns in neighboring positions at a level not lower than -2 dB . In this case, the width of the radiation patterns in the azimuthal plane (XOY in Figure 12) is approximately 62° , in the meridional plane 16° , and the gain of the annular antenna array is in the range of 14,5-15 dB.

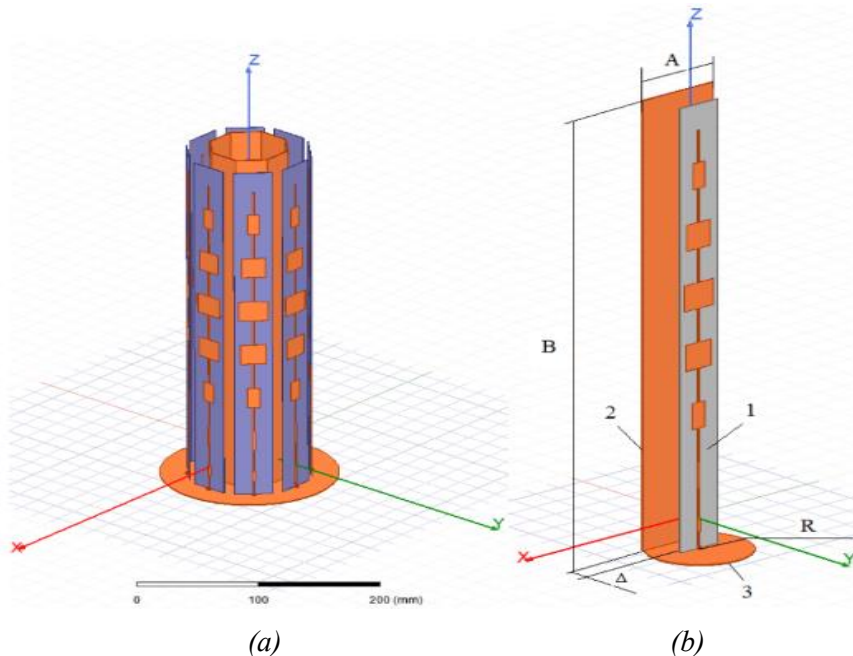


Figure 10. Eight-element circular microwave antenna array (a), single array element (b).

Radial structure is the structure of the arrangement of elements in the antenna array, in which the emitters are evenly placed on circles of a certain radius. We will call the increment of circle radius $r=100\text{ mm}$ a step along the radial coordinate. The emitters are evenly distributed on the circle with a step along the angular coordinate. The antenna array radius is 100 mm, the reflector radius is 85 mm, the reflector height is 50 mm and the screen radius is 135 mm. It is essential that due to the optimization of the width of the patches in the

vertical arrays, the level of the side lobe patterns of the annular antenna array in the meridional plane in the operating frequency band does not exceed - 21,7 dB.

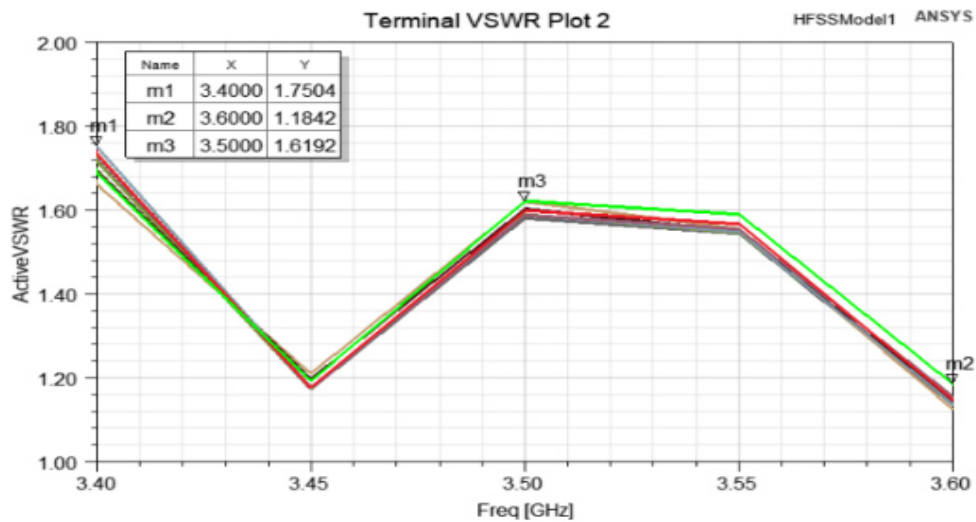


Figure 11. Frequency characteristics of the active standing wave ratio at the inputs of the annular antenna array.

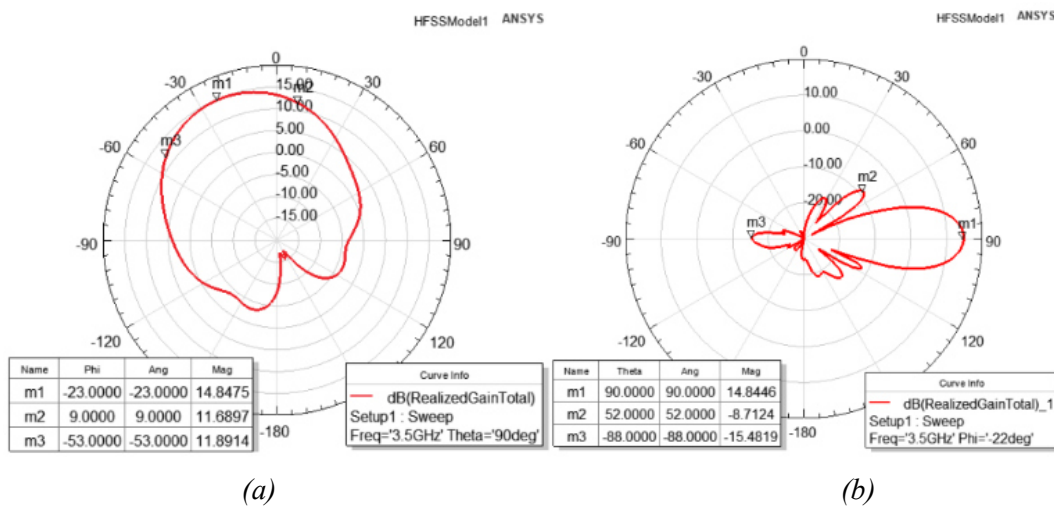


Figure 12. Azimuthal (a) and meridional (b) radiation patterns of an annular antenna array at a frequency of 3,5 GHz for the case of two active elements.

On Figure 13 shows the radiation patterns of the ring antenna array in the mode of equal-amplitude in-phase excitation of all eight vertical linear arrays. As can be seen from Figure 13 (a), the annular antenna array has an almost circular azimuthal radiation pattern.

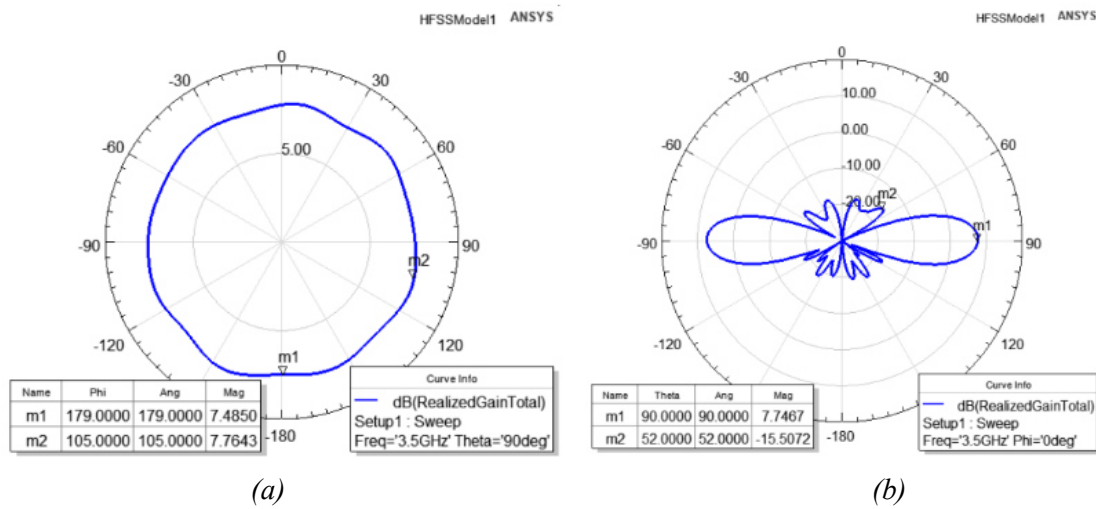


Figure 13. Azimuthal (a) and meridional (b) radiation patterns of an annular antenna array at a frequency of 3,5 GHz when all eight elements are excited.

Thus, the considered strip ring antenna array can operate in two modes - with a fixed circular or scanning sector radiation pattern with a fairly high gain and a low level of side radiation.

8 Analysis of the characteristics of the proposed antenna array

Calculation of the coefficient of the annular antenna array system is carried out by summing the electromagnetic fields of all individual radiation elements. In this case, for each study element located in the plane of the annular antenna array at a point with coordinates x_n, y_n , phase incursion is calculated by the formula:

$$\psi = 57,3 \cdot k \cdot (x_n \cdot \sin(v) \cdot \cos(v) \cdot \sin(\phi)) \quad (1)$$

where k is the wave number; x_n, y_n – emitter location coordinates along the X -axis (azimuthal plane) and along the Y -axis (elevation plane), respectively; ϕ is the angle between the y and z axes, the vector is orthogonal to the projection onto the yz plane (Figure 14); ϑ is the angle between the x axis and the yz plane. The location of the angles ϑ and ϕ is shown in Figure 14.

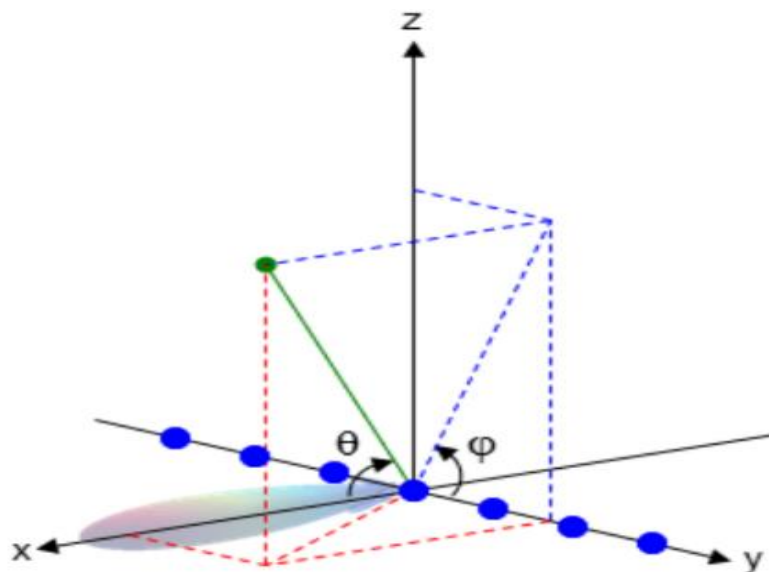


Figure 14. The location of the angles between the x, y and z axes of the coordinate system.

Analysis of the influence of electrical scanning on the parameters of the antenna array was carried out on a flat multi-element active phased antenna array. The array uses signal transmission paths with discrete phase shifters, the discrete is 5,625 degrees. The analysis was carried out in a computer-aided design system using the finite element method. Below are the results of the analysis in graphical form: the calculated radiation patterns of the annular antenna array with a uniform phase distribution (Figure 15), as well as the radiation patterns when the main beam is deflected by 0,02; 5; 20; 45 and 60 degrees in the azimuthal plane (Figures 16-20 respectively). In the elevation plane, the results are not given, since according to the technical specifications, the deviation is required within ± 10 degrees, which does not require adjustment.

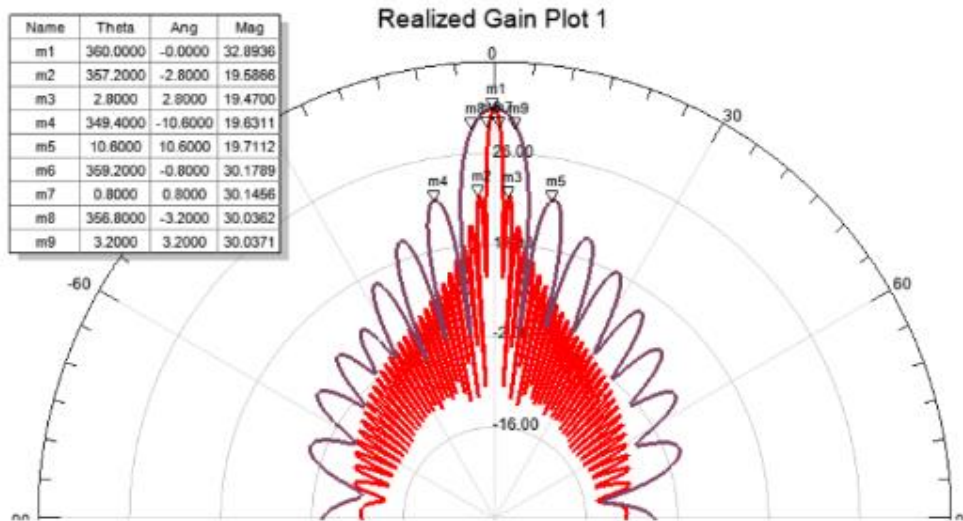


Figure 15. Antenna array radiation pattern with a beam deflection of 0,02 degrees.

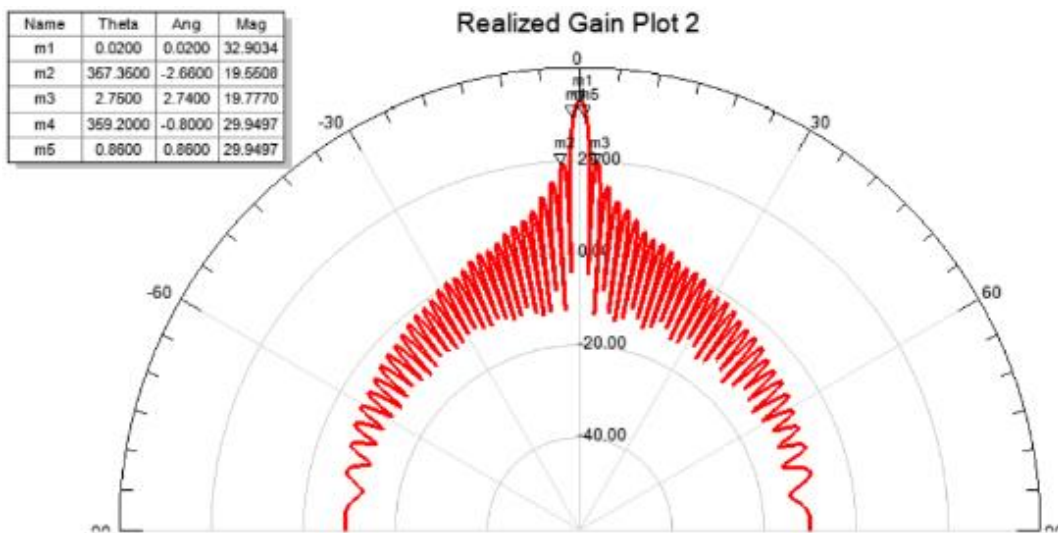


Figure 16. Antenna array radiation pattern with uniform phase distribution.

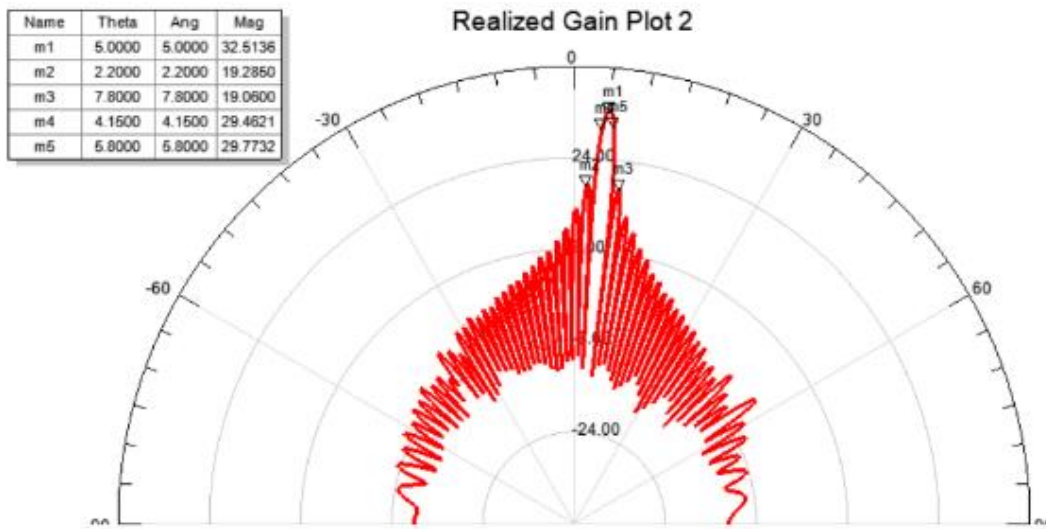


Figure 17. Antenna array radiation pattern with a beam deflection of 5,0 degrees.

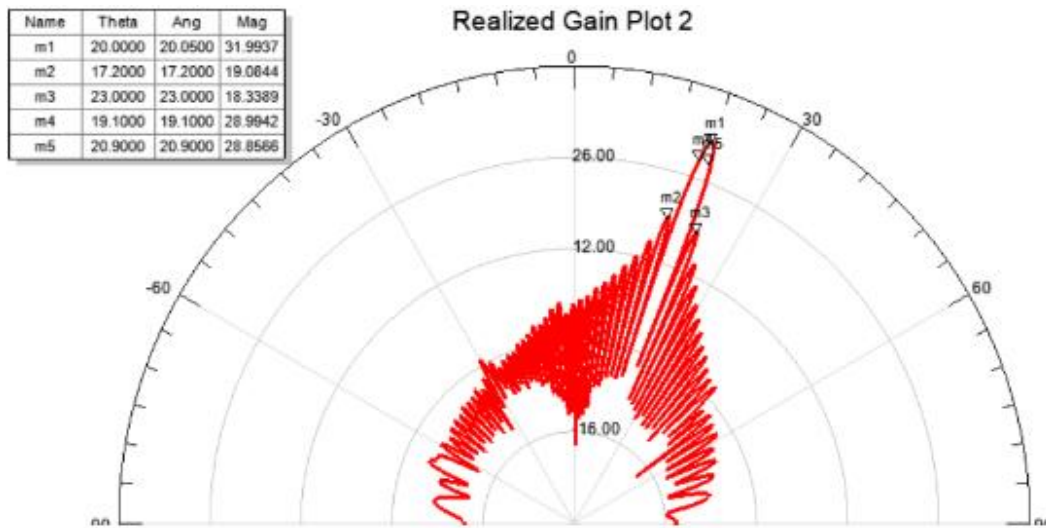


Figure 18. Antenna array radiation pattern with a beam deflection of 20,0 degrees.

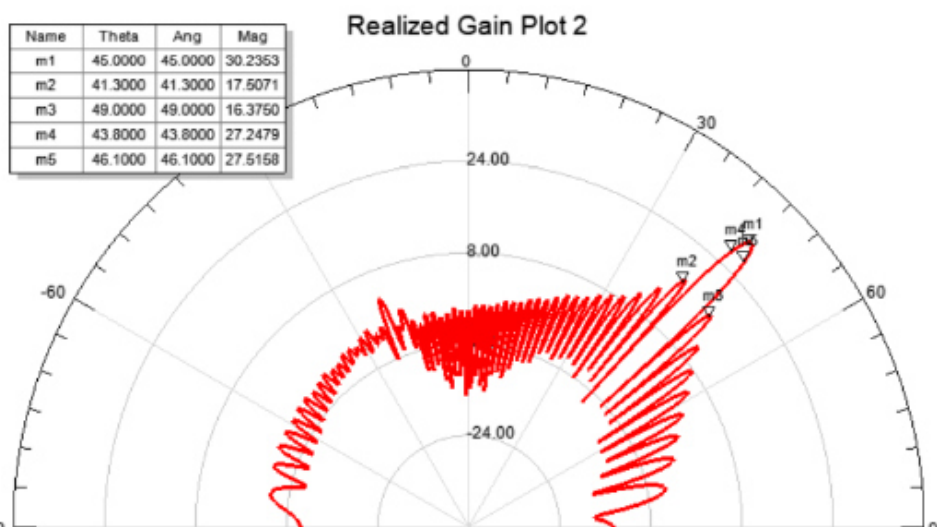


Figure 19. Antenna array radiation pattern with a beam deflection of 45,0 degrees.

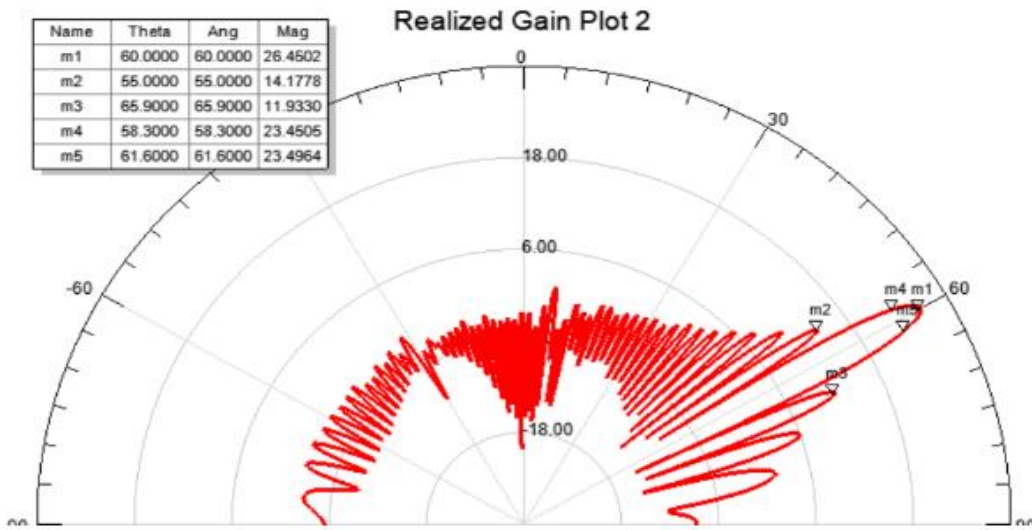


Figure 20. Antenna array radiation pattern with a beam deflection of 60,0 degrees.

Figure 15 shows sections of the radiation pattern of the antenna array at a frequency of 9 GHz in azimuth and elevation. Further analysis was carried out only in azimuth, due to the small number of emitters in elevation. As can be seen, when the main beam deviates from the normal, the characteristics of the radiation pattern change. As can be seen from Figure 15, the deviation of the beam from the normal due to electronic scanning directly affects the width of the main and the levels of the side lobes of the antenna beam. When the beam is deflected up to 60 degrees, the gain drops by 6,45 dB, the level of the side lobe deteriorates by 1 dB, and the width of the main lobe at a level of 0,5 more than doubles. To correct the characteristics of the radiation pattern, it is proposed to use the amplitude distribution of the electromagnetic field strength cosine square on the pedestal, since it is it that is the most variable in terms of choosing the height of the pedestal:

$$A_n m = \left(\Delta x + (1 - \Delta x) \cos^2 \left(\frac{\pi}{2} - \frac{\pi n}{N - 1} \right) \right) \times \left(\Delta y + (1 - \Delta y) \cos^2 \left(\frac{\pi}{2} - \frac{\pi m}{M - 1} \right) \right) \quad (2)$$

where $\Delta x, \Delta y$ are the height of the pedestal along the x and y axes, respectively; n, m is the distance between the centers of emitters located along the x and y axes, respectively; N, M are the number of emitters located along the x and y axes, respectively.

To analyze the influence of the amplitude distribution on the characteristics of the antenna, fixed values of the pedestal were taken along the X axis: 0,5; 0,3; 0,15; 0,1; along the Y axis: 0,5; 0,3; 0,1; 0,05; 0,01. The electromagnetic field strength calculations for each case were made using the Matlab software. An electromagnetic analysis of the antenna array to evaluate the characteristics of the radiation pattern was carried out in a computer-aided design system using the finite element method. The results of the analysis are summarized in Table 1 for convenience. As can be seen from Table 1, the height of the pedestal along the X and Y axes can influence the above listed main characteristics of the radiation pattern. Obviously, the desire to reduce the level of the side lobes affects the gain and the width of the main lobe, but it is this dependence that is proposed to be used in order to correct the radiation pattern. It is necessary to determine the initial cosine-square amplitude distribution on the pedestal for a uniform phase distribution, then analyze the distortion of the characteristics of the calculated phase distributions for beam rotation. The choice of pedestal height for each beam direction will determine the final characteristics of the antenna web. For clarity, Figure 21 shows a graphical representation of the amplitude distribution of the cosine square on a pedestal of 0,01 along the Y axis and 0,1 along the X axis.

Table 1. The results of the calculation of the amplitude distribution of the electromagnetic field.

Type of amplitude distribution of the electromagnetic field	Pedestal height		Gain, dB	Side lobe level, dB		Width of the main petal, °	
	Y axis	X axis		az	me	az	me
Uniform	-	-	33,0	13,3	13,0	1,7	6,59
Cosine squared on pedestal	0,51	0,51	32,9	16,3	17,0	1,7	6,39
	0,31	0,31	32,2	19,2	20,1	2,0	6,38
	0,11	0,11	31,6	23,69	28,4	2,1	8,28
	0,04	0,16	32,0	24,8	25,4	2,2	7,88
	0,045	0,17	31,6	24,6	28,9	2,2	8,1
	0,012	0,11	31,4	24,1	28,3	2,1	8,2

It follows from Figure 21 that the given number of emitters in the elevation plane (8 pcs.) limits the possibilities for implementing amplitude distributions. Increasing the number of radiators is one way to improve the accuracy of beam pattern correction results.

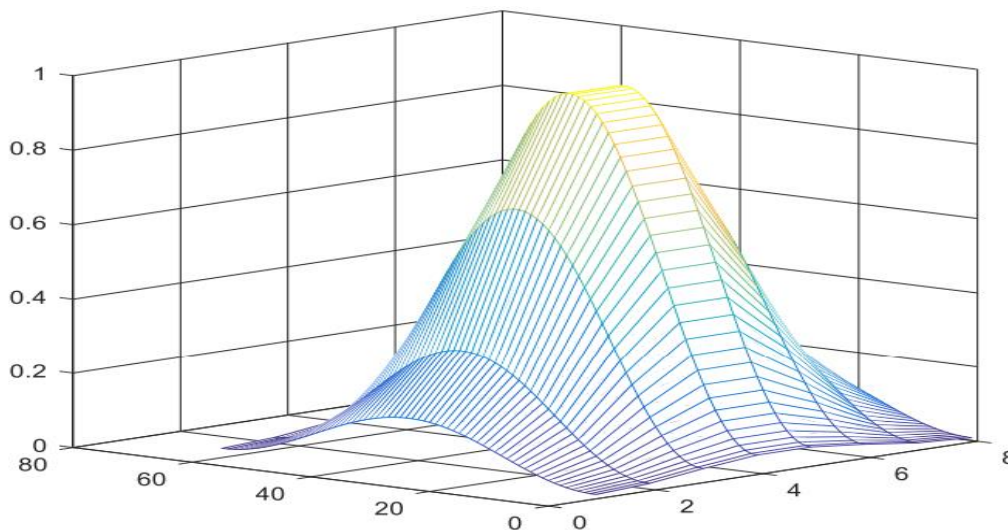


Figure 21. Graphical display of the amplitude distribution cosine square on a pedestal.

9 Comparisons of simulation and measurement results

The [30] features a sixteen-element, four-branch, dual-band microstrip antenna array. Dual band antenna array is suitable for ISM/Bluetooth/Zigbee/WiMAX/WiFi-2.4/5/6GHz applications. The antenna consists of eight round patch elements ($r = 2\text{ mm}$) and eight rectangular patch elements ($1 \times 8\text{ mm}$), which are connected together to provide dual range and create suitable wide-bandwidth emission characteristics. Therefore, an array is a combination of heterogeneous elements. Initially, both time and frequency domain solvers of Computer Simulation Technology (CST) are used to justify the antenna performance, i.e., to evaluate the antenna gain, directivity, E -field, H -field and system efficiency. Antenna area $40 \times 40 \times 0.79\text{ mm}^3$. Rogers RT 5880 (lossy) is used as the substrate, and metal (copper) is used as the emitting layers. The evaluation results indicate that the proposed antenna array operates in two bands 2,20–3,18 GHz and 4,81–7,21 GHz with center operating frequencies of 2,54 GHz and 5,64 GHz, respectively. It maintains return loss below -10 dB with better gain and directivity in both operating bands. The main purpose of using an antenna array is to obtain a compact antenna array with improved gain and also obtain dual band mode so that it can be used in various applications in daily life. The performance of the proposed antenna array is verified by three professional 3D electromagnetic simulators: High Frequency Structure Simulator (HFSS), FEKO (Computational

Electromagnetics Software) and CST. This [31] investigates uni-/multi-cast and orbital angular momentum (OAM) mode data transmission in orthogonal directions by the utilization of a new circular antenna array, operating at 28 GHz. In the horizontal plane the proposed antenna array operates as multimode transmitter (i.e., it provides broad-, uni- and/or multi-cast communication), while in the vertical direction OAM transmission occurs (i.e., it is capable of generating up to 15 spatially orthogonal OAM modes). Antenna array is designed using twelve, low-complexity, electromagnetically coupled microstrip patch antennas with high radiation efficiency. Each of these can transmit power of equivalent order of magnitude in both horizontal (i.e., broadside radiation pattern) and vertical direction (i.e., endfire radiation pattern) over electromagnetic waves of orthogonal electric components.

This property leads to the formation of uni-/multi-cast and OAM modes in the horizontal plane and vertical direction, respectively. Antenna was tested through full-wave electromagnetic analysis and measurements in terms of impedance matching, mutual coupling and radiation pattern: good agreement between simulated and measurement results was observed. Specifically, it presents up to 8,65 dB and 6,48 dB realized gain under the uni-cast (in the horizontal plane) and OAM mode (in the vertical plane), respectively. The proposed antenna array is perfect candidate for high spectral efficiency data transmission for 5G and beyond wireless applications, where orthogonality in communication links and OAM multiplexing is a requirement. To validate the obtained simulation results, it is necessary to compare the simulation and measurement results. Comparisons of the simulation and measurement results are made in Table 2. As can be seen from Table 2, the simulation and measurement results are in very good agreement. This confirms the reliability of the obtained modeling results.

Table 2. Comparisons of simulation and measurement results.

Characteristic	The simulation results	The measurement results
VSWR	1,02	1,04
Reflection coefficient	0,0099	0,0095
Antenna gain, dB	44,42	44,36

10 Conclusion

The obtained results suggest that the considered variants of the microwave ring antenna array with discrete-switching scanning of the azimuthal radiation patterns, taking into account the weight, size and electrical characteristics, seem promising for use in the equipment of radio communication, radar and radio control systems. And also a method for correcting the distortions of the directional patterns of the developed annular antenna array, caused by the mutual influence of emitters, is proposed. To implement this technique, an algorithm has been developed for changing the amplitude distribution of the electromagnetic field strength from the phase distribution of the electromagnetic field strength to compensate for the distortion of parameters caused by the deviation of the beam of the radiation pattern. When developing the algorithm, the following initial data were taken into account: the number of rays, the minimum scanning step, and the accuracy of the beam setting. It should be noted that the main components of radar stations are a transceiver or receiving module, a signal processing board, and an antenna device. The last node is always antenna arrays or aperture antennas due to high requirements for directional and energy characteristics. In order to increase the range of any radar or its sensitivity at a given distance, it is necessary to improve the signal-to-noise ratio, which can be achieved in several ways. Therefore, the results obtained in this work can be used for the antenna array of a radar system and radio direction finding.

Acknowledgement

The author expresses their deep gratitude to the entire editorial board of the journal for their professionalism and excellent work. I especially want to note the very careful and attentive attitude of the reviewers, and their

detailed study of the manuscript of the article. Their comments and recommendations are constructive, which allows for improving the quality of the presented research and structuring the article as much as possible according to the requirements of the journal. The friendly and prompt nature of communication with the editorial board contributes to the rapid resolution of all emerging issues and compliance with the stated deadlines for reviewing and publishing the article.

Funding

This work is supported by the author.

Declaration of interests

The author reports no conflict of interest.

Data availability statement

The data that support the findings of this study are available from the corresponding author, Elmar Hunbataliyev, upon reasonable request.

References

- [1] G. Kerim, and B. Suad, "A quantized water cycle optimization algorithm for antenna array synthesis by using digital phase shifters," *International Journal of RF and Microwave Computer-Aided Engineering*, vol. 25(1), 2015, pp. 21-29. (Journal article).
- [2] H. I. Taisir, and M. H. Zoubir, "Array Pattern Synthesis Using Digital Phase Control by Quantized Particle Swarm Optimization," *IEEE Transactions on Antennas and Propagation*, vol. 58(6), 2010, pp. 2142-2145. (Journal article).
- [3] P. David, O. Tamas, C. D. G. Deubauh, and K. N. Hamid, "Performance Comparison of Quantized Control Synthesis Methods of Antenna Arrays," *Electronics*, vol. 11(7), 2022, pp. 994-102.
- [4] S.-T. Sheu, J.-S. Wu, C.-H. Huang, Y.-C. Cheng, and L. Chen, "DDAS: Distance and Direction Awareness System for Intelligent Vehicles," *Journal of Information Science and Engineering*, vol. 23, 2007, pp. 709-722. (Journal article).
- [5] S. Liang, T. Feng, and G. Sun, "Sidelobe-level suppression for linear and circular antenna arrays via the cuckoo search-chicken swarm optimisation algorithm," *IET Microw. Antennas Propag.*, vol. 11, 2017, pp. 209-218. (Journal article).
- [6] H. Singh, B. S. Sohi, and A. Gupta, "Designing and performance evaluation of metamaterial inspired antenna for 4G and 5G applications," *Int. J. Electron.*, vol. 108, 2021, pp. 1035-1057. (Journal article).
- [7] H. Singh, N. Mittal, U. Singh, and R. Salgotra, "Synthesis of non-uniform circular antenna array for low side lobe level and high directivity using self-adaptive Cuckoo search algorithm," *Arab. J. Sci. Eng.*, vol. 47, 2022, pp. 3105-3118. (Journal article).
- [8] G. Yang, Y. Zhang, and S. Zhang, "Wide-band and wide-angle scanning phased array antenna for mobile communication system," *IEEE Open J. Antennas Propag.*, vol. 2, 2021, pp. 203-212. (Journal article).
- [9] R. Q. Wang, and Y. C. Jiao, "Synthesis of wideband rotationally symmetric sparse circular arrays with multiple constraints," *IEEE Antennas Wirel. Propag. Lett.*, vol. 18, 2019, pp. 821-825. (Journal article).
- [10] L. Hui, C. Yikai, and J. Ulrich, "Synthesis, Control, and Excitation of Characteristic Modes for Platform-Integrated Antenna Designs: A design philosophy," *IEEE Antennas and Propagation Magazine*, Vol. 64(2), 2022, pp. 41-48. (Journal article).
- [11] R. Castillo, R. Ma, and N. Behdad, "Platform-based electrically-small HF antenna with switchable directional radiation patterns," *IEEE Trans. Antennas Propag.*, vol. 69(8), 2021, pp. 4370-4379. (Journal article).
- [12] Y. Liu, J. Zhang, A. Ren, H. Wang, and C. Sim, "TCM-based heptaband antenna with small clearance for metal-rimmed mobile phone applications," *IEEE Antennas and Wireless Propag. Lett.*, vol. 18(4), 2019, pp. 717-721. (Journal article).

-
- [13] I. J. Islamov, E. G. Ismibayli, Y. G. Gaziyeu, S. R. Ahmadova, and R. S. Abdullayev, "Modeling of the Electromagnetic Field of a Rectangular Waveguide with Side Holes," *Progress in Electromagnetics Research*, vol. 81, 2019, pp. 127-132. (Journal article).
- [14] I. J. Islamov, N. M. Shukurov, R. S. Abdullayev, K. K. Hashimov, and A. I. Khalilov, "Diffraction of Electromagnetic Waves of Rectangular Waveguides with a Longitudinal," *IEEE Conferences 2020 Wave Electronics and its Application in Information and Telecommunication Systems*, 19806145, 2020, pp. 35-46. (Conference paper).
- [15] A. I. Khalilov, I. J. Islamov, E. Z. Hunbataliyev, N. M. Shukurov, and R. S. Abdullayev, "Modeling Microwave Signals Transmitted Through a Rectangular Waveguide," *IEEE Conferences 2020 Wave Electronics and its Application in Information and Telecommunication Systems*, 19806152, 2020, pp. 56-67. (Conference paper).
- [16] I. J. Islamov, and E. G. Ismibayli, "Experimental Study of Characteristics of Microwave Devices Transition from Rectangular Waveguide to the Megaphone," *IFAC-PapersOnLine*, vol. 51(30), 2018, pp. 477-479. (Conference paper).
- [17] E. G. Ismibayli, and I. J. Islamov, "New Approach to Definition of Potential of the Electric Field Created by Set Distribution in Space of Electric Charges," *IFAC-PapersOnLine*, vol. 51(30), 2018, pp. 410-414. (Conference paper).
- [18] I. J. Islamov, E. G. Ismibayli, M. H. Hasanov, Y. G. Gaziyeu, and R. S. Abdullayev, "Electrodynamics Characteristics of the No Resonant System of Transverse Slits Located in the Wide Wall of a Rectangular Waveguide," *Progress in Electromagnetics Research Letters*, vol. 8, 2018, pp. 23-29. (Journal article).
- [19] I. J. Islamov, E. G. Ismibayli, M. H. Hasanov, Y. G. Gaziyeu, S. R. Ahmadova, and R. S. Abdullayev, "Calculation of the Electromagnetic Field of a Rectangular Waveguide with Chiral Medium," *Progress in Electromagnetics Research*, vol. 84, 2019, pp. 97-114. (Journal article).
- [20] I. J. Islamov, E. Z. Hunbataliyev, and A. E. Zulfugarli, "Numerical Simulation of Characteristics of Propagation of Symmetric Waves in Microwave Circular Shielded Waveguide with a Radially Inhomogeneous Dielectric Filling," *International Journal of Microwave and Wireless Technologies*, vol. 9, 2021, pp. 761-767. (Journal article).
- [21] I. J. Islamov, M. H. Hasanov, and M. H. Abbasov, "Simulation of Electrodynamics Processes in a Cylindrical-Rectangular Microwave Waveguide Systems Transmitting Information," *11th International Conference on Theory and Application of Soft Computing, Computing with Words, Perception and Artificial Intelligence*, 2021, pp. 246-253. (Conference paper).
- [22] A. G. Charles, and Y. Guo, "A General Approach for Synthesizing Multibeam Antenna Arrays Employing Generalized Joined Coupler Matrix," *IEEE Transactions on Antennas and Propagation*, vol. 256, 2022, pp. 1-10. (Journal article).
- [23] A. K. Amin, "A Proposed Method for Synthesizing the Radiation Pattern of Linear Antenna Arrays," *Journal of Communications*, vol. 17(7), 2022, pp. 1-6. (Journal article).
- [24] A. Zeeshan, U. A. J. Zain, B. Shu-Di, and C. Meng, "Comments on Frequency Diverse Array Beampattern Synthesis with Taylor Windowed Frequency Offsets," *IEEE Antennas and Wireless Propagation Letters*, vol. 21(8), 2022, pp. 1713-1714. (Journal article).
- [25] Z. Wang, Y. Song, T. Mu, and Z. Ahmad, "A short-range range-angle dependent beampattern synthesis by frequency diverse array," *IEEE Access*, vol. 6, 2018, pp. 22664-22669. (Journal article).
- [26] X. Shao, T. Hu, Z. Xiao, and J. Zhang, "Frequency \pm synthesis with modified sinusoidal frequency offset," *IEEE Antennas Wireless Propag. Lett.*, vol. 20(9), 2021, pp. 1784-1788. (Journal article).
- [27] R. Quanxin, Q. Bingyi, C. Xiaoming, H. Xiaoyu, L. Qinlong, and Z. Jiaying, "Linear Antenna Array with Large Element Spacing for Wide-Angle Beam Scanning with Suppressed Grating Lobes," *IEEE Antennas and Wireless Propagation Letters*, vol. 21(6), 2022, pp. 1258-1262. (Journal article).
- [28] G. Yang, Y. Zhang, and S. Zhang, "Wide-band and wide-angle scanning phased array antenna for mobile communication system," *IEEE Open J. Antennas Propag.*, vol. 2, 2021, pp. 203-212. (Journal article).
- [29] Y.-F. Cheng, X. Ding, W. Shao, M.-X. Yu, and B.-Z. Wang, "A novel wide-angle scanning phased array based on dual-mode pattern reconfigurable elements," *IEEE Antennas Wireless Propag. Lett.*, vol. 16, 2017, pp. 396-399. (Journal article).

-
- [30] C. P. Liton, H. Ali, T. Rani, H. K. Saha, T. R. Jim, "A sixteen-element dual band compact array antenna for ISM/Bluetooth/Zigbee/WiMAX/WiFi-2.4/5/6 GHz applications," *Heliyon*, vol. 8(11), 2022, pp. 1-8. (*Journal article*).
- [31] S. D. Assimonis, M. A. B. Abbasi, V. Fusco, "Millimeter-wave multi-mode circular antenna array for uni-cast multi-cast and OAM communication," *Scientific Reports*, vol. 11, 2021, 4929, (*Journal article*).